Nanoscale Anionic Macromolecules Can Inhibit Cellular Uptake of Differentially Oxidized LDL

Evangelia Chnari,[‡] Jessica S. Nikitczuk,[†] Kathryn E. Uhrich,[§] and Prabhas V. Moghe*[,†,‡]

Department of Biomedical Engineering, Department of Chemical and Biochemical Engineering, and Department of Chemistry and Chemical Biology, Rutgers University, Piscataway, New Jersey 08854

Received September 19, 2005; Revised Manuscript Received December 13, 2005

Nanoscale particles could be synthetically designed to potentially intervene in lipoprotein matrix retention and lipoprotein uptake in cells, processes central to atherosclerosis. We recently reported on lipoprotein interactions of nanoscale micelles self-assembled from amphiphilic scorpion-like macromolecules based on a lauryl chloride−mucic acid hydrophobic backbone and poly(ethylene glycol) shell. These micelles can be engineered to present varying levels of anionic chemistry, a key mechanism to induce differential retentivity of low-density lipoproteins (LDL) (Chnari, E.; Lari, H. B.; Tian, L.; Uhrich, K. E.; Moghe, P. V. *Biomaterials* **2005**, *26*, 3749). In this study, we examined the cellular interactions and the ability of carboxylate-terminated nanoparticles to modulate cellular uptake of differentially oxidized LDL. The nanoparticles were found to be highly biocompatible with cultured IC21 macrophages at all concentrations examined. When the nanoparticles as well as LDL were incubated with the cells over 24 h, a marked reduction in cellular uptake of LDL was observed in a nanoparticle concentration-dependent manner. Intermediate concentrations of nanoparticles (10^{-6} M) elicited the most charge-specific reduction in uptake, as indicated by the difference in uptake due to anionic and uncharged nanoparticles. At these concentrations, anionic nanoparticles reduced LDL uptake for all degrees of oxidation (no oxidation, mild, high) of LDL, albeit with qualitative differences in the effects. The anionic nanoparticles were particularly effective at reducing the very high levels of uptake of the most oxidized level of LDL. Since complexation of LDL with anionic nanoparticles is reduced at higher degrees of LDL oxidation, our results suggest that anionic nanoparticles interfere in highly oxidized (hox) LDL uptake, likely by targeting cellular/receptor uptake mechanism, but control unoxidized LDL uptake by mechanisms related to direct LDL−nanoparticle complexation. Thus, anionically functionalized nanoparticles can modulate the otherwise unregulated internalization of differentially oxidized LDL.

Introduction

Atherosclerosis, the occlusive artery disease, is associated with the accumulation of lipid-laden macrophages, called foam cells, within the artery wall.[2] It is the primary cause of heart disease and stroke and the major underlying cardiovascular pathology for nearly half of all adult deaths in Western societies.[3] Elevated serum cholesterol, particularly in the form of apolipoprotein B-containing lipoproteins, is an important etiological factor in the pathogenesis of atherosclerosis.[4−6] The rate of development of atherosclerotic lesions depends greatly on the lipoprotein−arterial wall interactions. One of the factors that accelerate the atherogenic process is believed to be LDL modification within the arterial wall, specifically LDL oxidation, which leads to unregulated cellular uptake of the modified LDL in the earliest stages of the development of atherosclerotic plaques.[7,8] Early atherogenesis is accompanied by the formation of fatty streaks that consist of a subendothelial collection of foam cells derived from cholesterol-laden macrophages or smooth muscle cells.[9]

Low-density lipoproteins (LDLs) are the major carriers of cholesterol in the blood plasma and enter the arterial wall through the injured endothelium, or through areas of arterial branching.[3,10] In the intima, LDLs are sequestered by extracellular matrix molecules, mainly proteoglycans, and get further chemically and oxidatively modified before release, whereupon they can interact with intimal macrophages. Depending on the degree of oxidative modification, LDL interacts with macrophages through different sets of receptors, which has significant consequences on the nature and rate of LDL uptake processes. Unoxidized (native) LDL is steadily and slowly internalized mainly through the LDL receptor via clathrin-mediated endocytosis, a pathway that is controlled by a feedback inhibition mechanism, leading to down-regulation of cell surface receptors when intracellular cholesterol levels increase. Oxidized LDL uptake, in contrast, is more rapid and is mediated by scavenger receptors, such as scavenger receptor A (SR-A),[11−14] scavenger receptor B (SR-B), and CD36,[15−17] as well as CD68,[18] all of which lead to uncontrolled lipoprotein uptake and accumulation of cholesteryl esters in the cytoplasm,[14,19,20] thus contributing to foam cell formation.[20,21]

In this study it is hypothesized that anionic nanoparticles designed with differential LDL-retentive properties can modulate LDL uptake by macrophages to control unregulated intracellular LDL accumulation. We have designed a family of nanoparticles (Figure 1) based on amphiphilic micellar macromolecules self-assembled from unimers containing (i) methoxy-terminated poly(ethylene glycol) (PEG), contributing to the hydrophilicity and flexibility of the polymer, as well as to controlled protein repulsion, (ii) mucic acid, a multihydroxylated saccharide providing reaction sites for polymer modification, and (iii) aliphatic chains of varying lengths for control of the polymer hydrophobicity and aggregation behavior. We have previously

* Corresponding author. Phone: 732-445-4951. Fax: 732-445-2581. E-mail: Moghe@rci.rutgers.edu.
† Department of Biomedical Engineering.
‡ Department of Chemical and Biochemical Engineering.
§ Department of Chemistry and Chemical Biology.

10.1021/bm0506905 CCC: $33.50
Published on Web 01/13/2006

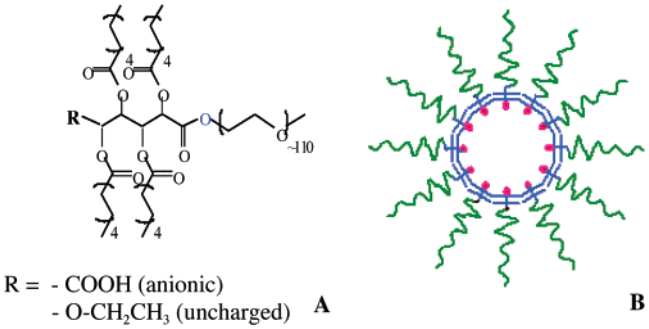

Figure 1. Schematic of the structure of the amphiphilic nanoparticles. The nanoparticle unit ($M_{12}P_5$ macromolecule) (A) consists of three biocompatible building blocks, PEG, mucic acid, and alkyl chains, and spontaneously forms micelles in solution (B) for concentrations above the critical micelle concentration (cmc = 10^{-7} M). For the uptake studies, two different chain end functionalities, carboxylic groups as anionic nanoparticles and ethoxy groups as uncharged (control) nanoparticles, were evaluated as shown in part A.

shown that carboxylate-terminated nanoparticles (termed, anionic nanoparticles) can successfully recapitulate the interactions between charged anionic matrix molecules such as glycosaminoglycans and differentially oxidized LDL.[1] Specifically, the anionic nanoparticles retain native and mildly oxidized LDL but not highly oxidized LDL.[1] The respective uncharged nanoparticle controls do not exhibit any affinity for LDL at any degree of oxidation. Utilizing the same nanoparticles in this study, the interactions between differentially oxidized LDL and nanoparticles were carefully evaluated for further influence on the LDL uptake behavior by IC21 macrophages. The IC21 macrophage system has already been evaluated as an effective and appropriate model to study atherogenic processes; cell exposure to modified lipoproteins elicits reactive oxygen intermediate production and apoptosis.[22] We report that the anionic nanoparticles can sensitively control the LDL cellular uptake as a function of the degree of LDL oxidation.

Materials and Methods

Lipoprotein Model−LDL Oxidation. Fluorescently labeled low-density lipoprotein (LDL-BODIPY) purified from human plasma (Molecular Probes, Eugene, OR) was employed for all the experiments in this study. Differentially oxidized LDL was obtained and characterized via methods elaborated in an earlier study.[1] In brief, mild LDL oxidation was achieved by incubating 50 μg/mL LDL with 10 μM $CuSO_4$ at 37 °C for 2 h.[23,24] Highly oxidized LDL was generated by incubating 50 μg/mL LDL with 10 μM $CuSO_4$ at 37 °C for 18 h exposed to air.[23,25] In all cases, oxidation was terminated with an aqueous solution of 0.01% w/v ethylenediaminetetraacetic acid (EDTA) (Sigma, St. Louis, MO). The extent of LDL oxidation was characterized by the content of conjugated dienes,[26,27] lipid peroxides,[28] and thiobarbituric acid reactive substances (TBARS)[26,29] as well as by monitoring LDL relative electrophoretic mobility (REM), which correlates with the overall change in the LDL particle charge.[30,31] In our experiments, the REM values for mildly oxidized LDL and highly oxidized LDL were 1.5 and 3.6, respectively, compared to REM of 1.0 for native LDL.[1]

Interactions between Nanoparticles and LDL. Details about the synthesis of the amphiphilic micellar nanoparticles employed in our investigation were previously published.[1,32,33] The macromolecules that form the micellar nanoparticles consist of a hydrophobic segment of mucic acid with pendant lauryl chloride chains and a hydrophilic segment of poly(ethylene glycol) (Figure 1). Carboxylate-terminated polymers were used as model anionic nanoparticles, whereas methoxy-terminated polymers were used as uncharged control nanoparticles.[1] All products were characterized by nuclear magnetic resonance and mass spectroscopy (for chemical composition) as well as gel permeation chromatography (for macromolecular size and size dispersity).

Critical micelle concentration (cmc) measurements were performed by fluorescence spectroscopy and determined to be 10^{-7} M for both anionic and uncharged nanoparticles.[32,33] Dynamic light scattering (DLS) was utilized to determine the micelle size and distribution—the nanoparticles were unimodal and very stable upon dilution. Interactions between the nanoparticles and LDL were studied at a nanoparticle concentration of 10^{-4} M, which is well above the cmc. These polymeric micelles were incubated with 10 μg/mL LDL at 37 °C for 12 h to reach equilibrium. Samples were then analyzed using dynamic light scattering (DLS) to examine the formation of LDL−nanoparticle complexes.[1] As previously described,[1] the DLS analysis was performed on aqueous nanoparticle solutions via photon correlation spectroscopy using a PSS Nicomp 380 submicrometer particle sizer instrument (Particle Sizing Systems, Santa Barbara, CA), and data were analyzed using intensity weighted histograms.

Cell Culture Conditions. Nanoparticle and LDL uptake studies were conducted using mouse IC21 peritoneal macrophage cell line (IC21) (ATCC, Manassas, VA), which was propagated in culture using RPMI-1640 media (ATCC, Manassas, VA) containing 10% fetal bovine serum (FBS) (Gibco-Invitrogen, Carlsbad, CA) and 1% penicillin/streptomycin (Biowhittaker, Walkersville, MD). The cells were harvested at confluence, and 10 000 cells/well were recultured in 96-well tissue culture plates for 5 days, prior to experimental use. IC21 sublines were propagated for a maximum of 8 weeks.

Nanoparticle Exposure and Cellular Viability. The nanoparticle biocompatibility with the cells was investigated using the live/dead assay (Molecular Probes, Eugene, OR). This cell viability assay is based on the simultaneous determination of live and dead cells using two respective fluoroprobes: calcein-AM (green), which stains cells with plasma membrane integrity; and ethidium-homodimer (red), which stains the nuclei of dead cells lacking plasma and nuclear membrane integrity. Cells were cultured in 96-well Falcon tissue culture polystyrene plates (Fisher Scientific, Suwanee, GA) for 5 days prior to experiment. To identify the nanoparticle concentrations that may be potentially cytotoxic, the cells were incubated with increasing nanoparticle concentrations (from 10^{-8} to 10^{-4} M) for different time points (t = 1, 5, 24 h) in a 37 °C, humidified incubator. Then, cells were washed twice with Dulbecco's phosphate-buffered saline (DPBS) with Ca^{2+} and Mg^{2+} (Biowhittaker, Walkersville, MD) and stained for cell viability measurements. Images were captured with a computer-interfaced inverted LSM 410 Zeiss epifluorescence microscope (Sun Microsystems, Santa Clara, CA), and the percent of live cells compared to total cells was enumerated. Each condition was performed in triplicate, and 5 fields were captured per well.

Effect of Nanoparticle Concentration on LDL Uptake. Cells were incubated with 10 μg/mL of fluorescently labeled differentially oxidized LDL for 24 h at 37 °C in the absence or presence of varying concentrations (from 10^{-8} to 10^{-4} M) of anionic and uncharged nanoparticles. The cells were then washed, and fluorescent images were captured on a computer-interfaced inverted LSM 410 Zeiss epifluorescence microscope (Sun Microsystems, Santa Clara, CA) for determination of cell-associated fluorescence. Then, the cells were lysed, and the concentration of intracellular fluorescently labeled LDL was quantified. Results were normalized to mg of cell protein using the Lowry assay and correlated to the fluorescence intensity quantified via microscopy.

Cell Uptake Kinetics of LDL−Nanoparticles. The uptake behavior of fluorescently labeled LDL and nanoparticles by IC21 macrophages was investigated systematically at 37 °C. Briefly, 10 μg/mL fluorescently labeled LDL preincubated with anionic nanoparticles was incubated with IC21 cells for 2, 5, and 24 h, at 37 °C in a humidified incubator with 5% CO_2. Controls included incubations with equivalent concentrations of LDL in the absence of nanoparticles, as well as LDL in the presence of uncharged nanoparticles. The cells were, then, washed twice with serum-free RPMI containing 0.4% bovine serum albumin

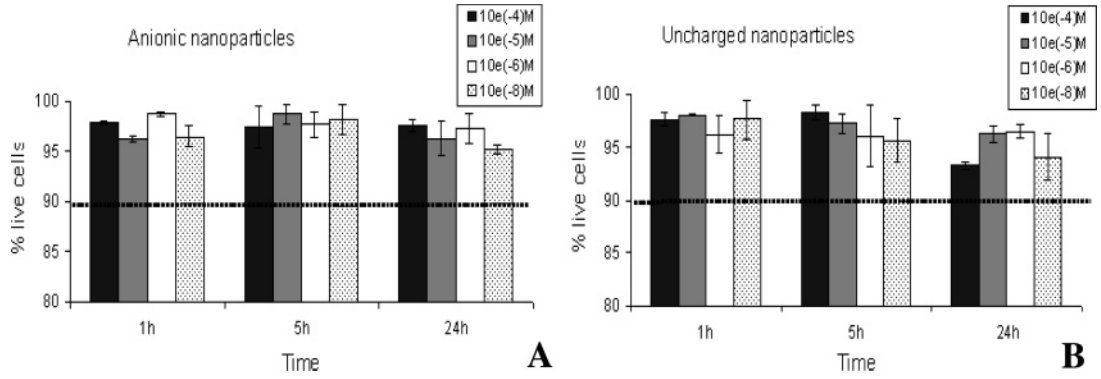

Figure 2. Biocompatibility studies of the nanoparticles with IC21 macrophages. Varying concentrations of (A) anionic and (B) uncharged nanoparticles were incubated with IC21 macrophages over time. The live/dead assay was performed to quantify cell survival after exposure to the nanoparticles. Data represent two independent experiments. Each experiment was evaluated in triplicate with 5−7 fields captured per condition.

(BSA) (Sigma, St. Louis, MO) and twice with serum-free RPMI. The cell-associated fluorescence was measured by capturing images on a confocal microscope (Sun Microsystems, Santa Clara, CA) and quantifying the fluorescence intensity using Image Pro Plus 5.1 software (Media Cybernetics, San Diego, CA). The cells were, then, lysed using 0.03 g of sodium dodecyl sulfate (SDS) (BioRad, Richmond, CA) in 30 mL of sodium hydroxide (NaOH, 0.1 N) (EM Science, Gibbstown, NJ). The internalized fluorescence was determined with fluorescence intensity measurements using the Cytofluor 4000 fluorescence multiwell plate reader (Applied Biosystems, Foster City, CA) and converted into concentration using a standard curve. The results were normalized per mg of cell protein that was determined using the modified Lowry protein assay (Pierce, Rockford, IL) and used in conjunction with the microscopy results to calculate differentially oxidized LDL uptake by macrophages.

Fluorescent Labeling of Nanoparticles. To elucidate the interactions of the nanoparticles with IC21 macrophages, the anionic nanoparticles were fluorescently labeled with cationic Texas red hydrazide dye (Molecular Probes, Eugene, OR) using carbodiimide chemistry. Briefly, to a polymer solution of anionic nanoparticles at a concentration of 10^{-4} M, 10^{-3} M of 1-ethyl-3-(3-dimethylaminopropyl)carbodiimide hydrochloride (EDC or EDAC) (Advanced ChemTech, Louisville, KY) and 10^{-3} M Texas red dissolved in *N*,*N*-dimethylformamide (DMF) (Sigma, St. Louis, MO) were added. The reactants were incubated overnight under stirring to maximize conjugation of the dye to the nanoparticles and evaporation of the organic solvent. The solution was then dialyzed against phosphate-buffered saline (PBS) at 4 °C for 24 h through 3500 MWCO regenerated cellulose dialysis tubing (wet in 0.1% sodium azide) (Spectrum Labs, Rancho Dominguez, CA), for removal of unbound Texas red and purification of the fluorescently labeled nanoparticles. Texas red in PBS in the absence of nanoparticles was used as a control throughout the process.

Uptake Studies of Fluorescently Labeled Nanoparticles and LDL-BODIPY by IC21 Macrophages. For cellular uptake studies, a 5% solution of the fluorescently labeled nanoparticles was mixed with nonfluorescent anionic or uncharged nanoparticles dissolved in serum-free RPMI (named after Roswell Park Memorial Institute, where it was developed). The nanoparticles were mixed with 10 μg/mL LDL overnight to allow for complexation. Then, the mixture was added to the cells and incubated for 5 h at 37 °C in a humidified incubator with 5% CO_2. After the incubation, the supernatant with the unbound nanoparticles and LDL was removed, and the cells were washed with serum-free RPMI and imaged using a LSM 410 Zeiss epifluorescence microscope (Sun Microsystems, Santa Clara, CA) at 80× magnification.

Results

Nanoparticle Interactions with Macrophages. To evaluate the possible cytotoxicity of the nanoparticles, IC21 macrophages were incubated with different concentrations of anionic and uncharged nanoparticles (Figure 1) in cell growth medium (RPMI-1640). The cellular viability data indicate that both anionic and uncharged nanoparticles are highly biocompatible with our cellular system, as more than 90% of the cells exposed to the nanoparticles survived even at the highest concentration of the nanoparticles (Figure 2). The nanoparticle biocompatibility did not considerably decrease with exposure time up to 24 h and was not sensitively dependent on the nanoparticle concentration.

To investigate the interactions between the nanoparticles and macrophages, we fluorescently labeled the carriers with Texas red and monitored their uptake by the cells. Confocal *z*-sectioning of the cells showed internalization of the nanoparticles, which was a function of nanoparticle concentration (data not shown).

Effect of the Nanoparticle Concentration on LDL Uptake. The effect of nanoparticle concentration on the LDL−cell interactions was quantified for differentially oxidized LDL (Figure 3). For nanoparticle concentrations above the critical micelle concentration (cmc), LDL uptake was significantly reduced with increasing nanoparticle concentration, which signifies competitive uptake between nanoparticles and LDL. Nanoparticle concentrations below the cmc (10^{-7} M) did not have a significant effect on LDL uptake, implying the importance of the 3-D presentation and clustering of the anionic charges in the efficiency of the LDL uptake inhibition. For all LDL oxidative states, a significant decrease in the LDL uptake in the presence of nanoparticles was observed that was more pronounced in the case of the anionic nanoparticles. The most prominent effect of the anionic charges on the inhibition of LDL uptake was observed for nanoparticle concentration of 10^{-6} M. Higher nanoparticle concentrations appeared to mask the specific inhibitory effect of the carboxyl groups of the nanoparticles. The difference in the inhibitory capacity of the anionic nanoparticles compared to that of the uncharged ones increased with increasing LDL oxidation.

LDL Uptake Studies in IC21 Macrophages. The effect of anionic or control nanoparticles on the time course of the macrophage internalization was evaluated using differentially oxidized LDL. The data of intracellular LDL concentration normalized to the cellular protein content is plotted in Figure 4. For all oxidative states of LDL, the uptake by macrophages was markedly decreased in the presence of both anionic and uncharged nanoparticles compared to that of LDL alone. Overall, the inhibition of LDL uptake was significantly greater for the anionic nanoparticles and the effect was more prominent with increasing LDL oxidation. To visually confirm this effect, the nanoparticles were fluorescently labeled with Texas red and

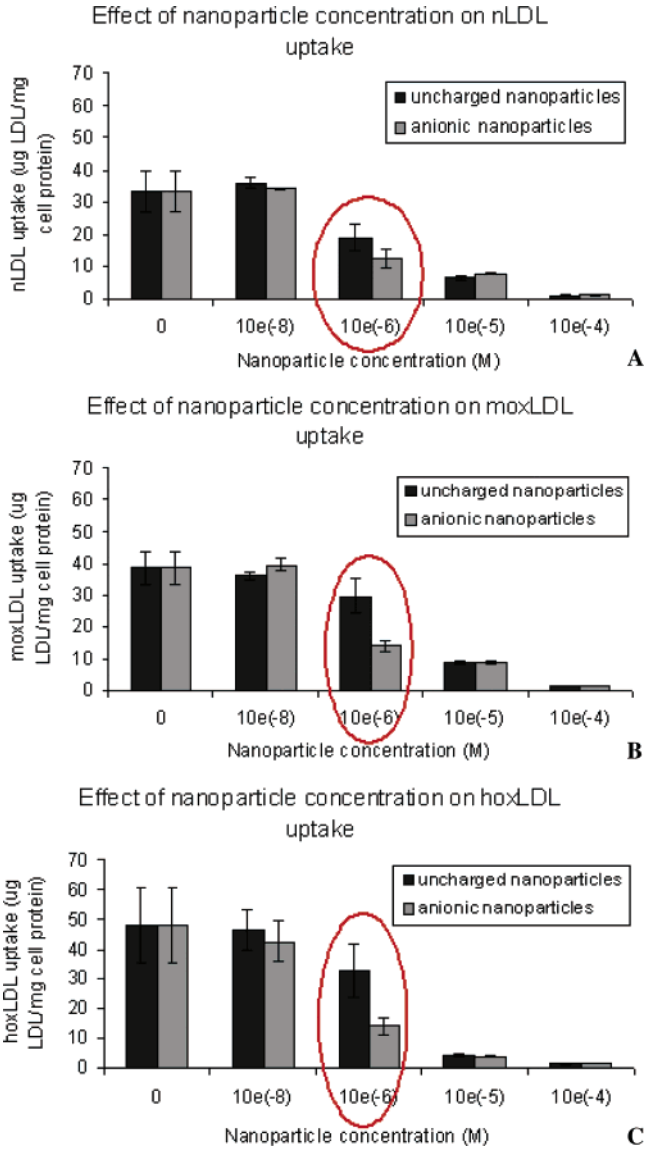

Figure 3. Effect of nanoparticle concentration on the uptake of differentially oxidized LDL. Anionic and uncharged nanoparticles were prepared at a range of concentrations (from 10^{-8} to 10^{-4} M) and incubated with 10 μg/mL (A) native, (B) mildly oxidized, and (C) highly oxidized LDL overnight. They were, then, added to IC21 macrophages, and LDL uptake was quantified after 24 h. The circled conditions represent the most sensitive condition (10^{-6} M) that shows the effect of uncharged and, more importantly, anionic nanoparticles in reducing LDL uptake. The results were normalized to mg of cell protein using the Lowry assay. Results represent 2−3 independent experiments per condition. Experiments were done in triplicate. Statistical analysis was conducted with ANOVA single factor ($P < 0.05$).

high-magnification images were captured of the cell association for nanoparticles and green fluorescent LDL (Figure 5 A−D). Simultaneous addition of LDL and nanoparticles to the cells led to reduced cell-associated LDL (green fluorescence) compared to that of LDL alone for both types of nanoparticles and LDL oxidative states. In the case of native LDL, the presence of uncharged (Figure 5G) and anionic nanoparticles (Figure 5E) causes similar decrease in LDL uptake. The yellow fluorescence observed mainly at the anionic nanoparticle condition (Figure 5E) represents colocalization of LDL (green) and nanoparticles (red), associated with complexation of the two. For highly oxidized LDL, the uncharged nanoparticles (Figure 5H) cause a basal reduction in the green fluorescence (LDL uptake), which is significantly further reduced in the presence of anionic nanoparticles (Figure 5F). The prominent red fluorescence signifies enhanced nanoparticle−cell interactions that may potentially be blocking the hoxLDL internalization. Lack of prominent yellow fluorescence in this case represents the lack of interactions between hoxLDL and the nanoparticles.

Discussion

The uncontrolled uptake of oxidized forms of LDL by the cells of the vascular intima is one of the most significant determinants of the escalation of atherogenesis. The interactions between LDL and cells are, in turn, governed by the retention behavior of LDL by charged matrix molecules, the glycosaminoglycans. In a previous study,[1] we demonstrated that carboxyl-terminated amphiphilic nanoparticles (15−20 nm size) interact primarily with native and mildly oxidized LDL, forming complexes of around 60−90 nm in diameter. Notably, the carboxylated nanoparticles did not interact with highly oxidized LDL, a behavior consistent with proteoglycans that also display anionic functionalities and release highly oxidized, and consequently negatively charged, LDL.[23] The respective uncharged nanoparticle controls did not exhibit any affinity for LDL at any degree of oxidation. The major finding of our current report is that synthetic nanoparticles can be designed to present GAG-mimetic negative charges to differentially reduce the internalization of oxidized LDL within IC21 macrophages.

The basal uptake behavior of IC21 macrophages toward LDL was similar to those previously reported for other cell types, including murine peritoneal macrophages,[15,34] THP-1 cells,[34,35] and J774 macrophages,[36,37] although the absolute amounts of LDL internalization varied depending on cell type and oxidative conditions. Uptake of unoxidized LDL by macrophages in the absence of nanoparticles follows the typical pattern of regulated uptake reported for native LDL; when more highly oxidized LDL was examined, the degree of uptake and the kinetics of uptake were significantly enhanced.

The key finding of this study is that the synthetically designed anionic nanoparticles could significantly reduce the very rapid uptake of the highly oxidized LDL, which is the most pathogenic form of LDL. The reduction in uptake rate was maximal at early times (2 h) when almost 80% decrease in the uptake rate was observed. Notably, in our culture system, the basal uptake rate of highly oxidized LDL in the absence of any nanoparticles was very high early on (almost 5-fold that of unoxidized LDL), but it slowed by 24 h, indicating the significance of intervention early on. Future efforts will need to examine whether long term uptake rates of highly oxidized LDL are similarly affected by the anionic nanoparticles.

Although our studies do not address the mechanisms directly, the mechanism for nanoparticle-mediated inhibition of uptake of highly oxidized LDL and unoxidized LDL are likely to be distinct. As previously demonstrated,[1] highly oxidized LDL does not complex with either anionic or uncharged polymer. Thus, we hypothesize that the inhibitory effect of the anionic nanoparticles on the internalization of highly oxidized LDL is primarily due to the anionic nanoparticle interactions with the scavenger receptors mediating oxidized LDL uptake. One of the major receptors known to mediate highly oxidized LDL uptake is SR-A that binds to LDL principally, but not exclusively, via charge interactions.[30] A typical feature of the class A scavenger receptors is that they mediate the uptake and degradation of several polyanionic ligands and modified proteins.[11] As LDL gets progressively oxidized, the positive charge on the ϵ-amino groups of the apolipoprotein B-100 in LDL can

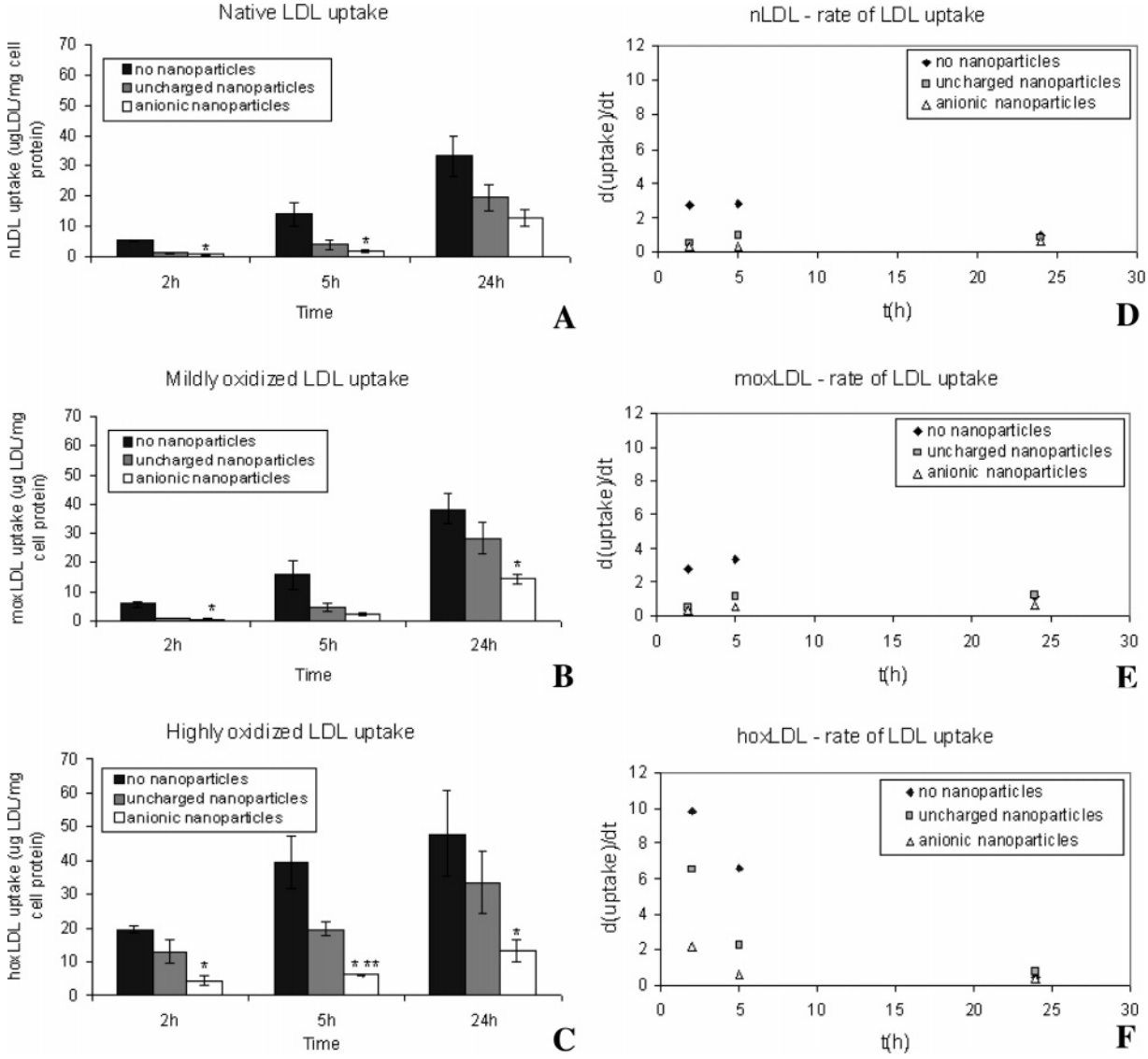

Figure 4. Inhibition of differentially oxidized LDL uptake by IC21 macrophages. Cells were incubated with (A) native, (B) mildly oxidized, and (C) highly oxidized LDL for 2, 5, and 24 h, in the presence and absence of 10^{-6} M anionic and uncharged nanoparticles. Fluorescent images were captured before the cells were lysed, and intracellular fluorescently labeled LDL was quantified. The results were normalized to mg of cell protein using the Lowry assay. The changes in the rate of LDL uptake over time (D−F) were calculated as $\Delta C/\Delta t$. Results represent 2−3 independent experiments per condition. Experiments were performed in triplicate. Statistical analysis was conducted with ANOVA single factor ($P < 0.05$). * represents significant difference compared to the no nanoparticle control and ** compared to the uncharged nanoparticle control.

get neutralized, thereby increasing the net negative charge of LDL,[46] thus converting it into a major ligand for this scavenger receptor. SR-A is a ligand for many polyanionic molecules that are not structurally related.[12,46] The anionic nanoparticles could, thus, interact with the scavenger receptor, blocking highly oxidized LDL binding and uptake. Current studies are ongoing to explore the role of both scavenger receptor and nonscavenger receptor mechanisms mediating nanoparticle uptake by macrophages (Chnari et al., in preparation). Future studies on LDL uptake will need to focus on systematically examining the role of the nature and density of anionic groups displayed from the nanoparticles, as well as the cooperative roles of the nanoparticle core properties (hydrophobicity, flexibility, degree of PEGylation).

It is noteworthy that despite the distinct carrier-retention behaviors of unoxidized and highly oxidized LDL, which have been previously documented,[1] significant inhibition of cell uptake of all differentially oxidized forms of LDL was observed in our current study. We believe this behavior can be explained by two different modes of inhibition. For unoxidized LDL, the anionic nanoparticles readily complex with LDL and, thus, compete with native LDL receptor for binding to LDL. In contrast, for highly oxidized LDL, no complexation is reported between anionic nanoparticles and LDL; the anionic nanoparticles compete with LDL for binding to the scavenger receptors. Mildly oxidized LDL exhibits a combined fate: it is internalized via scavenger receptors, but it can also be complexed to the anionic nanoparticles; thus, the mechanism of inhibition is likely a combination of competition with both the receptors (for binding to LDL) as well as with LDL (for binding to the receptors). In the case of unoxidized LDL, the anionic nanoparticles form complexes with LDL, and the reduced LDL uptake could be explained either by steric hindrance for binding to the LDL receptor or by slower diffusion, due to the bigger size of the LDL−nanoparticle complexes compared to that of single LDL particles. Studies comparing large versus small particles of LDL uptake and degradation by fibroblasts have shown that fewer large LDL particles are catabolized than small particles, although large LDL binds with higher affinity to the receptor than small LDL.[38] Chappell et al.[38] proposed a lattice

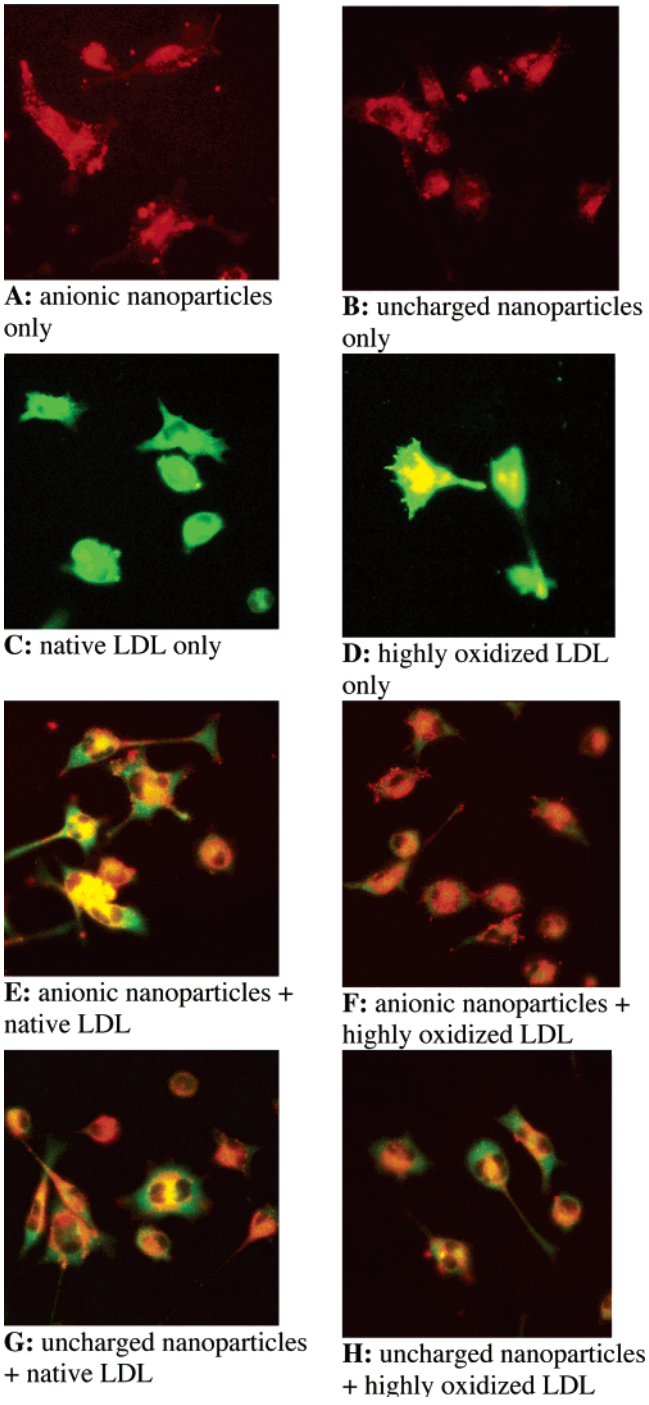

Figure 5. Visualization of the role of nanoparticles in inhibiting native and highly oxidized LDL uptake. Anionic (A) and uncharged (B) nanoparticles were fluorescently labeled with Texas red and incubated with native and highly oxidized LDL to allow for complexation. Native LDL uptake was considerably reduced in the presence of both the anionic (E) and the uncharged nanoparticles (G) compared to the condition where no nanoparticles were added (C). The uncharged nanoparticles also had a basal effect in inhibiting highly oxidized LDL uptake (H), but the inhibition was more dramatic in the presence of anionic nanoparticles (F), compared to that of hoxLDL in the absence of nanoparticles (D).

model to describe LDL catabolism via the LDL receptor pathway, wherein the ligand size plays an important role in receptor-mediated binding and cellular uptake. Similarly, the internalization of nanoparticle-complexed LDL in this study may be diminished due to the increased size of the LDL−nanoparticle complexes (60−90 nm) compared to that of uncomplexed LDL (22 nm).[1] This hypothesis is further supported by the clathrin coated pits' (e.g., LDL receptor pathway) and caveolae (e.g., SRB-I pathway) capacity to bind particles of sizes up to 200 nm and less than 1 μm, respectively.[39] For a certain capacity in these invaginations, fewer large particles (complexes) than smaller particles (uncomplexed LDL) would fit. The significantly reduced internalization of complexed native LDL compared to that of uncomplexed LDL could also be attributed to the steric hindrance for LDL binding to the native LDL receptor, since the receptor binding site on LDL is proximal to the charge-sensitive site on LDL for binding to the nanoparticles.[4,40−42] Similarly, binding of LDL to proteoglycans shields the positively charged domains required for interaction with the LDL receptor.[43]

Notably, the uncharged nanoparticles also lowered differentially oxidized LDL uptake, although significantly less than the anionic nanoparticles. This effect may represent the baseline of the nonspecific inhibition for LDL uptake due to introduction of certain molecules in the system. When isolating the interactions of the nanoparticles with cells in the absence of any LDL, both anionic and neutral nanoparticles were observed to be directly taken up by macrophages (Figure 5, parts A and B), which may occur concomitantly and possibly competitively with the binding and uptake of LDL or LDL−nanoparticle complexes. These interactions may have a more pronounced effect at higher nanoparticle concentrations, as supported by the data presented in Figure 3. Preliminary experiments aimed at clarifying the nanoparticle−cell interactions indicate that none of the receptors examined (LDL receptor, scavenger receptor A, CD36, SRBI/II) mediated the uptake of uncharged nanoparticles within IC21 macrophages, whereas SRA receptors were partially involved in the uptake of anionic nanoparticles (Chnari et al., in preparation). Thus, uncharged particles are likely internalized via nonreceptor-mediated pathways, potentially lipid rafts[44,45] or pinocytosis (nonspecific internalization of small particles), so their inhibitory effect may represent the blocking of these nonspecific routes of LDL internalization.

Studies are currently under way to identify the specific receptor-mediated pathways involved in the inhibitory effect of the anionic nanoparticles in oxidized LDL uptake by macrophages. Insights from such studies could aide in the development of synthetic nanoparticles as efficient receptor blockers for controlled oxidized LDL uptake. Future efforts will also need to examine the physicochemical properties of the nanoparticles (size, amphiphilicity, location of charge display) that may be important to high-potency binding to receptors.

Acknowledgment. This study was supported by an NSF-BES (0201788) Grant, an American Heart Association Grant-in-Aid (9951060T; 0455823T) award to P. Moghe, and an NSF-BES (9983272) Grant to K. E. Uhrich. We thank Dr. Lu Tian and Jinzhong Wang (Department of Chemistry and Chemical Biology, Rutgers University) for the synthesis of the nanoparticles we used in our studies.

References and Notes

(1) Chnari, E.; Lari, H. B.; Tian, L.; Uhrich K. E.; Moghe P. V. *Biomaterials* **2005**, *26*, 3749−58.
(2) Patel, R. P.; Moellering, D.; Murphy-Ullrich, J.; Jo, H.; Beckman, J. S.; Darley-Usmar, V. M. *Free Radical Biol. Med.* **2000**, *28*, 1780−94.
(3) Lusis, A. J. *Nature* **2000**, *407*, 233−241.
(4) Skalen, K.; Gustafsson, M.; Rydberg, E. K.; Hulten, L. M.; Wiklund, O.; Innerarity, T. L.; Boren, J. *Nature* **2002**, *417*, 750−4.
(5) Saini, H. K.; Arneja, A. S.; Dhalla, N. S. *Can. J. Cardiol.* **2004**, *20*, 333−46.
(6) Choy, P. C.; Siow, Y. L.; Mymin, D.; O, K. *Biochem. Cell Biol.* **2004**, *82*, 212−24.

(7) Dhaliwal, B. S.; Steinbrecher, U. P. *Clin. Chim. Acta*. **1999**, *286*, 191−205.
(8) Camejo, G.; Olsson, U.; Hurt-Camejo, E.; Baharamian, N.; Bondjers, G. *Atheroscler. Suppl.* **2002**, *3*, 3−9.
(9) Young, I. S.; McEneny, J. *Biochem. Soc. Trans.* **2001**, *29*, 358−62.
(10) Gimbrone, M. A., Jr. *Thromb. Haemostasis* **1999**, *82*, 722−6.
(11) Yla-Herttuala, S.; Hiltunen, T. P. *Atherosclerosis* **1998**, *137* (Suppl), S81−8.
(12) de Winther, M. P.; van Dijk, K. W.; Havekes, L. M.; Hofker, M. H. *Arterioscler., Thromb. Vasc. Biol.* **2000**, *20*, 290−7.
(13) Hiltunen, T. P.; Yla-Herttuala, S. *Atherosclerosis* **1998**, *137* (Suppl), S81−8.
(14) Takahashi, Y.; Kinoshita, T.; Sakashita, T.; Inoue, H.; Tanabe, T.; Takahashi, K. *Adv. Exp. Med. Biol.* **2002**, *507*, 403−7.
(15) Lougheed, M.; Lum, C. M.; Ling, W.; Suzuki, H.; Kodama, T.; Steinbrecher, U. *J. Biol. Chem.* **1997**, *272*, 12938−44.
(16) Nicholson, A. C.; Han, J.; Febbraio, M.; Silversterin, R. L.; Hajjar, D. P. *Ann. N.Y. Acad. Sci.* **2001**, *947*, 224−8.
(17) Febbraio, M.; Sheibani, N.; Schmitt, D.; Silverstein, R. L.; Hajjar, D. P.; Cohen, P. A.; Frazier, W. A.; Hoff, H. F.; Hazen, S. L. *J. Clin. Invest.* **2000**, *105*, 1095−108.
(18) Ramprasad, M. P.; Terpstra, V.; Kondratenko, N.; Quehenberger, O.; Steinberg, D. *Proc. Natl. Acad. Sci. U.S.A.* **1996**, *93*, 14833−8.
(19) Berliner, J. A.; Heinecke, J. W. *Free Radical Biol. Med.* **1996**, *20*, 707−27.
(20) Brown, M. S.; Goldstein, J. L. *Annu. Rev. Biochem.* **1983**, *52*, 223−261.
(21) Steinberg, D. *J. Biol. Chem.* **1997**, *272*, 20963−20966.
(22) Rosenson-Schloss, R. S.; Chnari, E.; Brieva, T. A.; Dang, A.; Moghe, P. V. *Exp. Biol. Med*. **2005**, *230*, 40−8.
(23) Oorni, K.; Pentikainen, M. O.; Annila, A.; Kovanen, P. T. *J. Biol. Chem.* **1997**, *272*, 21303−11.
(24) Terpstra, V.; Bird, D. A.; Steinberg, D. *Proc. Natl. Acad. Sci. U.S.A.* **1998**, *95*, 1806−11.
(25) Chang, M. Y.; Potter-Perigo, S.; Wight, T. N.; Chait, A. *J. Lipid Res.* **2001**, *42*, 824−833.
(26) Patel, R. P.; Boersma, B. J.; Crawford, J. H.; Hogg, N.; Kirk, M.; Kalyanaraman, B.; Parks, D. A.; Barnes, S.; Darley-Usmar, V. *Free Radical Biol. Med.* **2001**, *31*, 1570−81.
(27) Esterbauer, H.; Striegl, G.; Puhl, H.; Rotheneder, M. *Free Radical Res. Commun.* **1989**, *6*, 67−75.
(28) Jiang, Z. Y.; Hunt, J. V.; Wolff, S. P. *Anal. Biochem.* **1992**, *31*, 384−9.
(29) el-Saadani, M.; Esterbauer, H.; el-Sayed, M.; Goher, M.; Nassar, A. Y.; Jurgens, G. *J. Lipid Res.* **1989**, *30*, 627−30.
(30) Wang, X.; Greilberger, J.; Ratschek, M.; Jurgens, G. *J. Pathol.* **2001**, *195*, 244−50.
(31) Jurgens, G.; Hoff, H. F.; Chisolm, G. M., III; Esterbauer, H. *Chem. Phys. Lipids* **1987**, *45*, 315−36.
(32) Tian, L. Novel Amphiphilic Macromolecules for Drug Delivery Applications: Design, Synthesis and Characterization. In *Department of Chemistry and Chemical Biology*; Rutgers, The State University of New Jersey: New Brunswick, NJ, 2004; p 171.
(33) Tian, L.; Yam, L.; Zhou, N.; Tat, H.; Uhrich, K. E. *Macromolecules* **2004**, *37*, 538−543.
(34) Wang, X.; Greilberger, J.; Ledinski, G.; Kager, G.; Jurgens, G. *J. Cell. Biochem.* **2001**, *81*, 557−69.
(35) Sugano, R.; Yamamura, T.; Harada-Shiba, M.; Miyake, Y.; Yamamoto, A. *Atherosclerosis* **2001**, *158*, 351−7.
(36) Hakamata, H.; Miyazaki, A.; Sakai, M.; Matsuda, H.; Suzuki, H.; Kodama, T.; Horiuchi, S. *J. Lipid Res.* **1998**, *39*, 482−94.
(37) Hendriks, W. L.; van der Boom, H.; van Vark, L. C.; Havekes, L. M. *Biochem. J.* **1996**, *314*, 563−8.
(38) Chappell, D. A.; Fry, G. L.; Waknitz, M. A.; Berns, J. J. *J. Biol. Chem.* **1991**, *266*, 19296−302.
(39) Rejman, J.; Oberle, V.; Zuhorn, I. S.; Hoekstra, D. *Biochem. J.* **2004**, *377*, 159−69.
(40) Camejo, G.; Hurt-Camejo, E.; Wiklund, O.; Bondjers, G. *Atherosclerosis* **1998**, *139*, 205−22.
(41) Boren, J.; Olin, K.; Lee, I.; Chait, A.; Wight, T. N.; Innerarity, T. L. *J. Clin. Invest.* **1998**, *101*, 2658−64.
(42) Olsson, U.; Camejo, G.; Hurt-Camejo, E.; Elfsber, K.; Wiklund, O.; Bondjers, G. *Arterioscler., Thromb. Vasc. Biol.* **1997**, *17*, 149−55.
(43) Kaplan, M.; Williams, K. J.; Mandel, H.; Aviram, M. *Arterioscler., Thromb. Vasc. Biol.* **1998**, *18*, 542−53.
(44) Makoveichuk, E.; Castel, S.; Vilaro, S.; Olivecrona, G. *Biochim. Biophys. Acta* **2004**, *1686*, 37−49.
(45) Boren, J.; Lookene, A.; Makoveichuk, E.; Xiang, S.; Gustafsson, M.; Liu, H.; Talmud, P.; Olivecrona, G. *J. Biol. Chem.* **2001**, *276*, 26916−22.
(46) Zhang, H.; Yang, Y.; Steinbrecher, U. P. *J. Biol. Chem.* **1993**, *268*, 5535−42.

BM0506905